NUCLEI, PARTICLES, FIELDS, GRAVITATION, AND ASTROPHYSICS

PRECISION MEASUREMENT OF GRAVITATIONAL FREQUENCY SHIFT OF ELECTROMAGNETIC SIGNALS

© 2024 V. N. Rudenko^a,*, A. V. Belonenko^a, A. V. Gusev^a, F. S. Gurin^a, V. V. Kulagin^a, S. M. Popov^a, G. D. Manucharyan^{a,b}, M. V. Zakhvatkin^c, A. V. Kovalenko^d

^aSternberg State Astronomical Institute, Lomonosov Moscow State University, Moscow 119992, Russia

^bBauman Moscow State Technical University, Moscow 105005, Russia

^cKeldysh Institute of Applied Mathematics of the Russian Academy of Sciences, Moscow 125047, Russia

^dLebedev Physical Institute of the Russian Academy of Sciences, Moscow 119991, Russia

*e-mail: valentin.rudenko@gmail.com

Received August 08, 2024
Revised September 12, 2024
Accepted September 12, 2024

Abstract. Communication radio signals between an orbital spacecraft (SC) and a ground tracking station (GTS) experience a frequency shift proportional to the positional difference of their gravitational potentials. The effect constitutes an experimental basis of the general theory of relativity (GR) as one of the aspects of Einstein's equivalence principle (EEP). The article presents the results of precision measurement of the effect using frequency standards placed on the SC and GTS. Data from special "gravitational sessions" of radio communication accumulated during the "RadioAstron" (RA) space radio telescope mission in 2015–2019 were used. Scrupulous analysis of these data allows to confirm the correspondence between theory and experiment with high accuracy: the violation parameter (deviation from GR) was $1.57 \pm 3.96 \cdot 10^{-5}$.

DOI: 10.31857/S004445102411e063

1. INTRODUCTION

A significant recent achievement in experimental astronomy was the successful implementation of the Space Radio Telescope (SRT) "RadioAstron" project with the Spektr-R satellite, carrying a parabolic antenna with a diameter of ≈ 10 meters, which, together with groundbased antennas, formed an interferometer with a record baseline length of $\approx 350,000$ km. This, along with microwave frequency standards on the satellite and ground stations, led to an order of magnitude improvement in angular resolution of radio interferometric measurements [1]. During the entire existence of SRT, from 2011 to 2019, up to ten different astronomical programs were carried out on this instrument, reports of which are stored in the ASC LPI, and the results have been published in numerous articles by the scientific team of the "RadioAstron" group. The main purpose of the "RadioAstron" mission was to act as a space radio interferometer. However, other applications of this unique space-based instrument to fundamental physics problems have been under consideration since the design stage. Thus, attention

was drawn to using the space interferometer with frequency standards for testing relativistic effects of GR, in particular, for precise measurement of gravitational frequency shift of electromagnetic signals — an effect that forms the experimental basis of GR and represents Einstein's equivalence principle in one of its forms [2]. Analysis and schemes of such type of gravitational measurements within the "RadioAstron" mission are contained in work [3].

The experiment involved measuring and comparing the frequencies of the onboard (i.e. on the SC) and ground standards during the orbital evolution of the Spektr-R satellite. Hydrogen standards produced by the domestic company "Vremya-Ch" were used, the stability of which in terms of Alan dispersion was $\Delta f/f = 1 \cdot 10^{-14}$ at averaging time $\sim 10^2$ s.

Let us recall that the idea of a space experiment to measure the gravitational red shift ("redshift effect") was first realised in the Gravity-Probe A (GP-A)

¹⁾ https://www.vremya-ch.com/index.php/projects-ru/spaceapplications-ru/vch-1010-ru/index.html

mission (1976), where an H-standard was lifted to a height of 10⁴ km by a ballistic missile. At the apogee of its trajectory the frequency was compared with a similar ground-based maser. Information about frequency variations was transmitted via communication radio signals. For real-time compensation of the dominant first-order Doppler effect, a special technique was developed, combining one-way (1w) signals synchronized with the onboard standard and two-way (or loop) (2w) signals referenced to the ground standard. Subsequently, similar techniques were used in many space launches. The result of the GP-A experiment was the confirmation of GR with an accuracy of hundredth of a percent ($\approx 1.4 \cdot 10^{-4}$) [4, 5]. This result persisted for almost 40 years. Recently, reports from the "Gallileo" navigation satellite group have emerged about tightening this limit to $\approx 3 \cdot 10^{-5}$ [7, 6].

Let's compare the conditions of RA measurements with GP-A and Gallileo experiments. The fundamental differences are as follows. The first represented a one-time measurement without the possibility of repetition and data accumulation. The second was performed with extremely small orbital modulation of the redshift effect. Moreover, both were conducted in the near-Earth zone with a radius more than an order of magnitude smaller than the RA orbit's apogee. The latter is fundamentally important for testing such an aspect of EPP as its positional invariance.

In the "RadioAstron" mission, the Spektr-R spacecraft moved in an elongated orbit with high eccentricity $e \approx 0.9$, with a floating period of 7-9 days (Moon's influence), with an apogee of $\approx 3.5 \cdot 10^5$ km; The calculated value of the relative gravitational frequency shift between ground and onboard standards at the points designated for measurements (cyclogram) lay in the range of $(5.3 - 6.8) \cdot 10^{-10}$, which demonstrates a noticeable modulation of the shift along the orbit. For comparison, note that for the two Gallileo satellites that provided the results of works [6,7], the orbital modulation of the shift was an order of magnitude smaller (< 0.1). Overall, the orbital (kinematic) parameters of the "RadioAstron" SC were convenient for studying the redshift effect.

However, there is a circumstance that makes it difficult to perform such an experiment like GP-A. The [4, 5] technique developed for compensating the first-order Doppler effect requires simultaneous operation of SC in both modes — one-way 1w and

two-way 2w. In practice, during the RA mission, like in most other space projects, such capability was not provided. To maintain "real-time" compensation of the dominant first-order Doppler effect, it was necessary to resort to an operational mode with switching regimes. This significantly complicated the procedure of filtering the gravitational shift and estimating measurement errors. In work [4, 5] the question was not only about the accuracy of gravitational shift measurement but also about the correspondence of the measured value to GR prediction (which is important for selecting competing relativistic gravity theories). This circumstance was formalized by introducing a "deviation parameter" epsilon ε :

$$\frac{\Delta f_{grav}}{f} = \frac{\Delta U}{c^2} (1 + \varepsilon), \tag{1}$$

where $\Delta f_{grav}/f$ is the measured frequency gravitational shift, ΔU is the difference of gravitational potentials at signal transmission and reception points, c and ε are the speed of light and violation (deviation) parameter respectively.

According to GP-A experiment results, the estimation of ϵ is at the level of $\epsilon \sim 10^{-4}$. Thus, for more reliable confirmation of GR, experiments (measurements) that give smaller values of ϵ are of interest. To date, there are works analyzing measurements conducted by RA mission. In work [8] without real time compensation of first-order Doppler effect, based only on one-way data, $\delta\epsilon \approx 0.016$ was obtained. In work [9] with real time compensation, but without optimal series combination, $\delta\epsilon \approx 3 \cdot 10^{-4}$ was found. Both results are worse than GP-A. The authors of work [11] draw attention to the Rao-Cramer bound for estimating the accuracy of gravitational shift measurements, but illustrate this only with specific examples, without providing results of comprehensive analysis of all sessions.

This article presents an analysis of the set of gravitational sessions of the "RadioAstron" mission, taking into account the accumulated experience in processing gravitational data by the Russian group working as part of an international collaboration. The analysis was performed within the framework of the Likelihood principle with minimal use of a priori information. The methodology and data processing itself, including algorithms, have been repeatedly and thoroughly described in the publications of the author group listed in the references. A clear block diagram (flowchart) of sequential processing steps

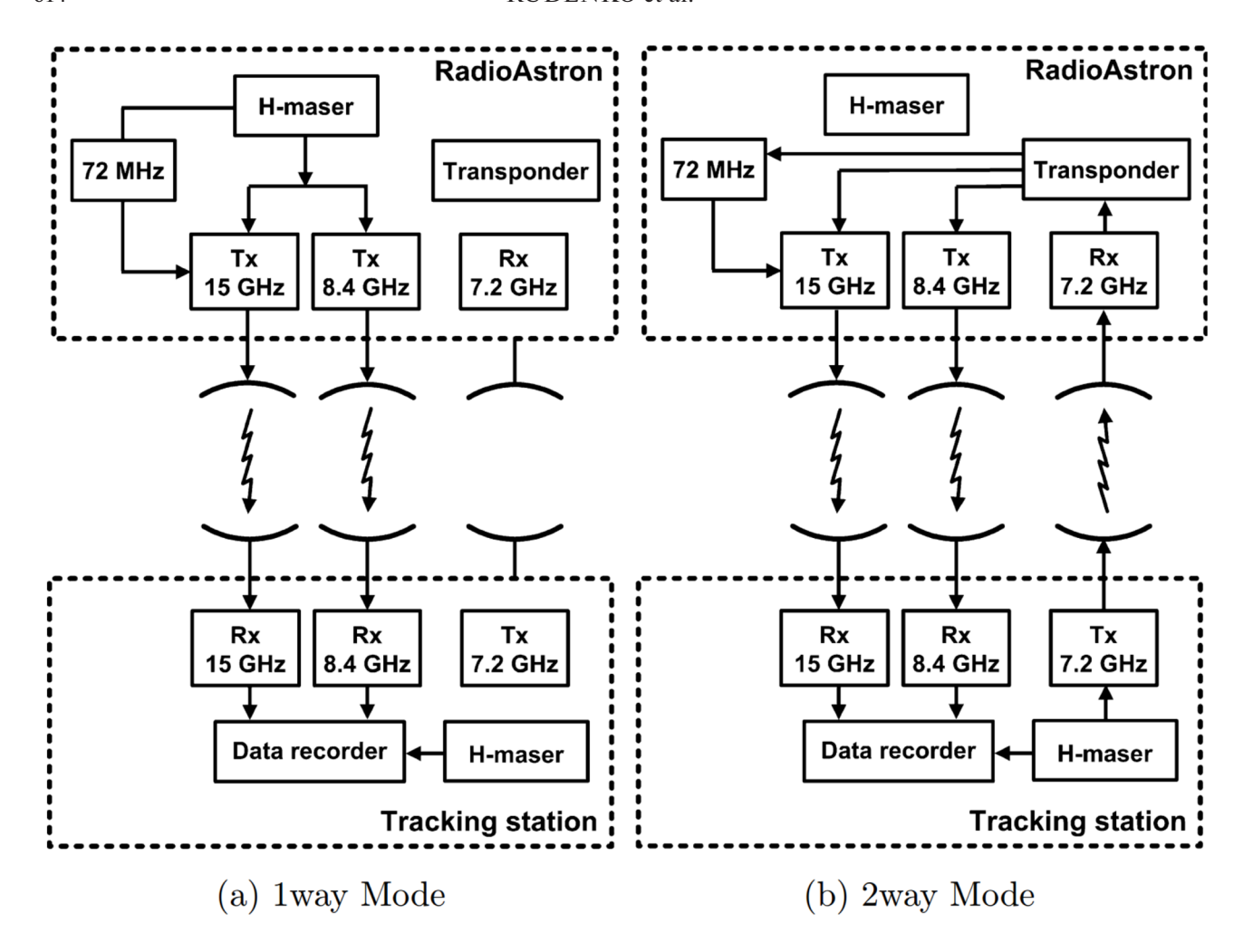


Fig. 1. RadioAstron spacecraft radio link operation modes: a — one-way, contains gravitational and Doppler frequency shifts; b — two-way, contains doubled Doppler shift and no gravitational shift. Explanations: H-maser — hydrogen frequency standard, Data recorder — recording device, Tx — transmitter, Rx — receiver, Tracking station — ground tracking station (GTS)

is contained, for example, in a recent article [9]. In addition to optimal filtering of useful information from the background of numerous physical noises in individual sessions, the procedure of optimal combination of the measurement data set was also performed. The result demonstrates the tightening of the violation (deviation) parameter boundary ε , lowering it to the level of $\sim 10^{-5}$.

2. MEASUREMENT STRATEGY

The main radio communication channels of the "RadioAstron" SRT had frequencies of 8.4 GHz and 15 GHz. For specialized gravitational sessions, scientific information was received at 8.4 GHz. The 15 GHz channel was primarily used for calibration measurements. As noted in the introduction, to maintain real-time compensation of the dominant

first-order Doppler shift, it was necessary to use an operational mode with changing synchronization modes (see Fig. 1). As a result, continuous recording of the communication signal becomes piecewise, consisting of segments referenced to onboard (1w) or groundbased (2w) standards (see Fig. 2). In order to obtain the desired filtration observable $\Delta f/f = (f_{1w} - 0.5f_{2w})/f$ [4], containing both modes at the same fixed time point, it is necessary to interpolate frequency data of mode 2w into the area between two adjacent segments (zone of existence of mode 1w), taking into account the interpolation error. Note here that operation in mode 2w had a technical peculiarity. The signal from the Ground Tracking Station is sent at an initial frequency of 7.2075 GHz, which is received on board the spacecraft with a correction for the Doppler effect. After heterodyning on the transponder, the signal is reflected down to the Ground Tracking Station

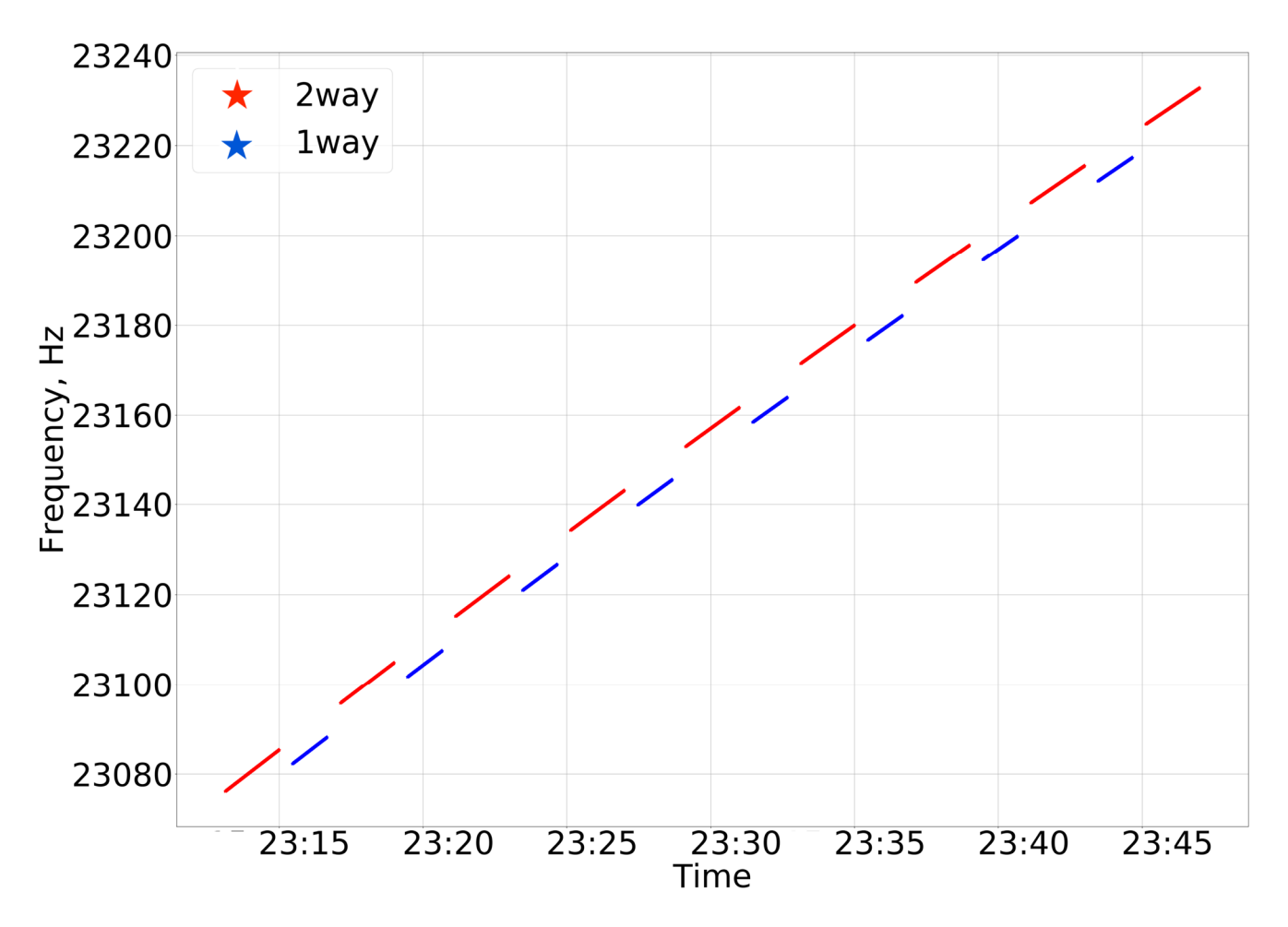


Fig. 2. Session raks 17bo (2016-12-15 23:00), alternation of synchronization mode zones 2w (red) and 1w (blue); mutual shift of tracks is due to the presence of gravitational shift in 1w data

at 8.4 GHz. New ground heterodyning translates the signal into the frequency range ≈ 6 MHz with subsequent digitization at 32 MHz and 2-bit amplitude quantization. To estimate the carrier frequency of the signal and its evolution during spacecraft movement, a known iterative "phase-stopping" algorithm was used, developed at the European institute for long-distance space communication JIVE, which includes gradual narrowing of the filter band, starting from 2 kHz [10]. Recording in mode 1w lasted 80 s, in mode 2w-120 s.

Data where the SNR of the received signal was less than 10^3 were excluded from processing. The algorithm is also described in more detail in article [11]. The typical duration of a gravitational session in practice was ≈ 40 min. To record the key compensation algorithm, let's introduce (define) the detuning of the transmitted signals. The relative frequency offset in oneway mode is

$$\Delta f_{1w}/f_{84} = (f_{1w} - f_{84})/f_{84},$$

where f_{1w} is the measured frequency in mode 1w, $f_{8.4}$ is the nominal frequency. The relative frequency offset in two-way mode, taking into account the Doppler effect correction, equals

$$\Delta f_{2w}/f_{8.4} = (f_{2w} - F_0 f_{up})/(F_0 f_{up}),$$

where $F_0 = 8.4/7.2075$ is the normalizing coefficient, f_{up} is the frequency at the moment of signal transmission from GS to SC. As a result, the key equation of the compensation scheme (GP-A) can be written as

$$\frac{\Delta f_{1w}}{f_{8.4}} - \frac{1}{2} \frac{\Delta f_{2w}}{f_{8.4}} = (1 + \varepsilon) \frac{\Delta U}{c^2} + \frac{\Delta f_{dop 2}}{f} + \frac{\Delta f_{Moon}}{f} + \frac{\Delta f_{Sun}}{f} + \frac{\Delta f_{nonsph}}{f} + \frac{\Delta f_{Atmosph}}{f} + \Delta h + o \left(\frac{v}{c}\right)^3, \quad (2)$$

where $\Delta U/c^2$ is the gravitational shift,

$$\frac{\Delta f_{dop2}}{f} = -\frac{|\mathbf{v}_e - \mathbf{v}_s|^2}{2c^2} + \frac{(\mathbf{D} \cdot \mathbf{a}_e)}{c^2}$$

– relativistic Doppler effect, $\Delta f_{Moon}/f$ – influence of the Moon's tidal potential, $\Delta f_{Sun}/f$ – influence of the Sun's tidal potential, $\Delta f_{nonsph}/f$ – influence of Earth's nonsphericity0, $\Delta f_{Atmosph}/f$ – atmospheric shift (including ionosphere and troposphere [12]), as well as flicker noise scintillation etc. [13], Δh is the effect of detuning (frequency mismatch) of frequency standards on SC and GS. Analysis showed that to measure ε with accuracy better than 10^{-4} , it is necessary to account for all effects with relative contribution greater than 10^{-14} . Below we discuss the influence of each effect listed in the main compensation scheme (2).

To measure the violation parameter with accuracy not worse than 10^{-5} it is necessary to account for the relativistic second-order Doppler effect. For this purpose, formulas from work [14] were used:

$$\frac{\Delta f_{dop2}}{f} = -\frac{|\mathbf{v}_e - \mathbf{v}_s|^2}{2c^2} + \frac{(\mathbf{D} \cdot \mathbf{a}_e)}{c^2}$$
(3)

 \mathbf{v}_e is the GS velocity, \mathbf{v}_s is the cSC velocity, \mathbf{D} is the distance vector from GS to SC, \mathbf{a}_e is the GS acceleration.

Note. All parameters in (3) must be converted to a unified EME2000 coordinate system. SC state vectors are provided by Keldysh Institute of Applied Mathematics in EME2000 system, Pushchino station state vectors had to be converted from ITRF (International Terrestrial Reference Frame) system to EME2000 system — this was done using the Earth rotation model adopted in IAU (International Astronomical Union) resolution and implemented in SOFA library [15].

It was also found that the relativistic Doppler effect has the greatest magnitude at distances up to 90,000 km, reaching $1.8 \cdot 10^{-10}$, which is comparable to the magnitude of the gravitational shift. The error in compensating for the relativistic Doppler effect is limited to $2 \cdot 10^{-16}$ and is caused by the error in velocity reconstruction ≈ 3 m/ms and position ≈ 300 m of the SC [16]. To evaluate the theoretical gravitational frequency shift $\Delta U/c^2$ a formula was

used that takes into account the correction for Earth's non-sphericity:

$$\frac{\Delta f_{grav}}{f} = \frac{\Delta U}{c^2} - \frac{G M_E R_E^2 J_2}{2r_s^3 c^2} (1 - \frac{3z_s^2}{r_s^2}) \tag{4}$$

 $\Delta U/c^2$ – the difference in Newtonian potentials of the GSS and SC, M_E – Earth's mass, R_E – Earth's radius, J_2 – quadrupole moment, z_s – spacecraft coordinate in the geocentric coordinate system, r_s – geocentric radius vector of the spacecraft, G – gravitational constant. Effects related to the tidal potential of the Moon and Sun were previously discussed in detail in article [17], the contribution of the ionosphere and troposphere was discussed in article [12], and the contribution of flicker noise in work [13]. The ordinal contribution of each effect is presented in Table 1 and Figure 3.

Concluding the description of the measurement strategy, we emphasize again that during gravitational sessions, the information signal was recorded continuously, but with jumps between operational modes 1w and 2w. During primary processing, we separated the signal into individual intervals with constant operation mode. Taking into account the session cyclogram, the non-stationary beginning of each interval 1w or 2w, where frequency capture occurred, was removed. Then, using a digital spectrometer, the frequency of the received signal was estimated (see details in work [11]). After the main compensation scheme 2 (first-order Doppler), finer compensation of residual effects was performed, whose ordinal contribution is presented in Table 1 and Figure 3.

Table 1. Residual effects after applying the main compensation scheme

Fine compensation effects				
Effect	max. value	error		
Grav. shift, $\Delta U/c^2$	$6.8 \cdot 10^{-10}$	$< 10^{-15}$		
Rel. Doppler effect, v^2/c^2	$1.8 \cdot 10^{-10}$	$< 10^{-16}$		
Grav. contribution of the Moon	$6 \cdot 10^{-13}$	< 10 ⁻¹⁶		
Grav. contribution of the Sun	$< 1 \cdot 10^{-14}$	$< 10^{-16}$		
$\Delta U/c^2$, quadrupole moment	$< 2 \cdot 10^{-15}$	$< 10^{-16}$		
$\Delta f_{ion}/f$ — ionospheric frequency shift	$<2\cdot10^{-14}$	< 10 ⁻¹⁶		
$\Delta f_{Trop}/f$ – tropospheric shift	$< 1 \cdot 10^{-15}$	< 10 ⁻¹⁶		
Flicker scintillation noise	$<1\cdot10^{-12}$	< 10 ⁻¹⁴		

Table 1 and Figure 3 show the results of random and systematic errors analysis with references in the text to works where this analysis is presented in detail. Recall that the influence of flicker effects was considered in papers [9, 13]. The interpolation error in the measurement mode with changing synchronization modes was calculated using polynomial approximation (scipy.interpolate) with preliminary modeling of the signal and main interference [9]. As a result, the error of the used interpolation did not exceed 10^{-4} Hz.

3. COMBINING SESSIONS

Our goal at the final stage was to estimate the violation parameter ε based on the totality of conducted gravitational sessions, corresponding to the maximum likelihood criterion. The entirety of measurement data can be described as a random process, represented by a discrete vector

$$\varepsilon = \|\varepsilon_1, \varepsilon_2, ..., \varepsilon_k\|^T$$

whose elements ε_k are estimates of parameter ε in each individual session.

With a sufficiently large number of sessions $k \gg 1$ (in the real experiment $k \approx 40$) and a very high signal-to-noise ratio: (SNR $\approx (10^5 \div 10^6)$) the distribution of parameter ε can be considered Gaussian and its estimation in session k can be written as $\varepsilon_k = \varepsilon \pm \Delta \varepsilon_k$,

where $\Delta \varepsilon_k$ are Gaussian random variables with parameters $\langle \Delta \varepsilon_k \rangle = 0$, such that $\langle \varepsilon_k \varepsilon_i \rangle = \sigma_k^2$ at k=i and 0 at $k \neq i$ ($\langle ... \rangle$ denotes statistical averaging). Under the condition of independent measurements in individual sessions and uncorrelated noise, the logarithm of the integral likelihood ratio of the vector process ε (for all sessions combined) splits into the sum of individual logarithms ε_k for each session, i.e., the following relations hold:

$$\ln \Lambda(\hat{\varepsilon} | \varepsilon) = \sum_{k=1}^{m} \ln \Lambda(\varepsilon_{k} | \varepsilon),$$

$$\ln \Lambda(\varepsilon_{k} | \varepsilon) = \frac{\varepsilon_{k} \varepsilon - \varepsilon^{2} / 2}{\sigma_{k}^{2}}.$$
(5)

The maximum likelihood integral estimate of the unknown parameter ε when combining all sessions is the solution to the extremum equation

$$\frac{\partial \ln \Lambda(\hat{\varepsilon}|\varepsilon)}{\partial \varepsilon} = 0, \tag{6}$$

hence, using equations (5), we can find the formula for optimal estimation ε :

$$\varepsilon_{opt} = \frac{\sum_{k=1}^{m} \frac{1}{\sigma_k^2} \varepsilon_k}{\sum_{k=1}^{m} \frac{1}{\sigma_k^2}},\tag{7}$$

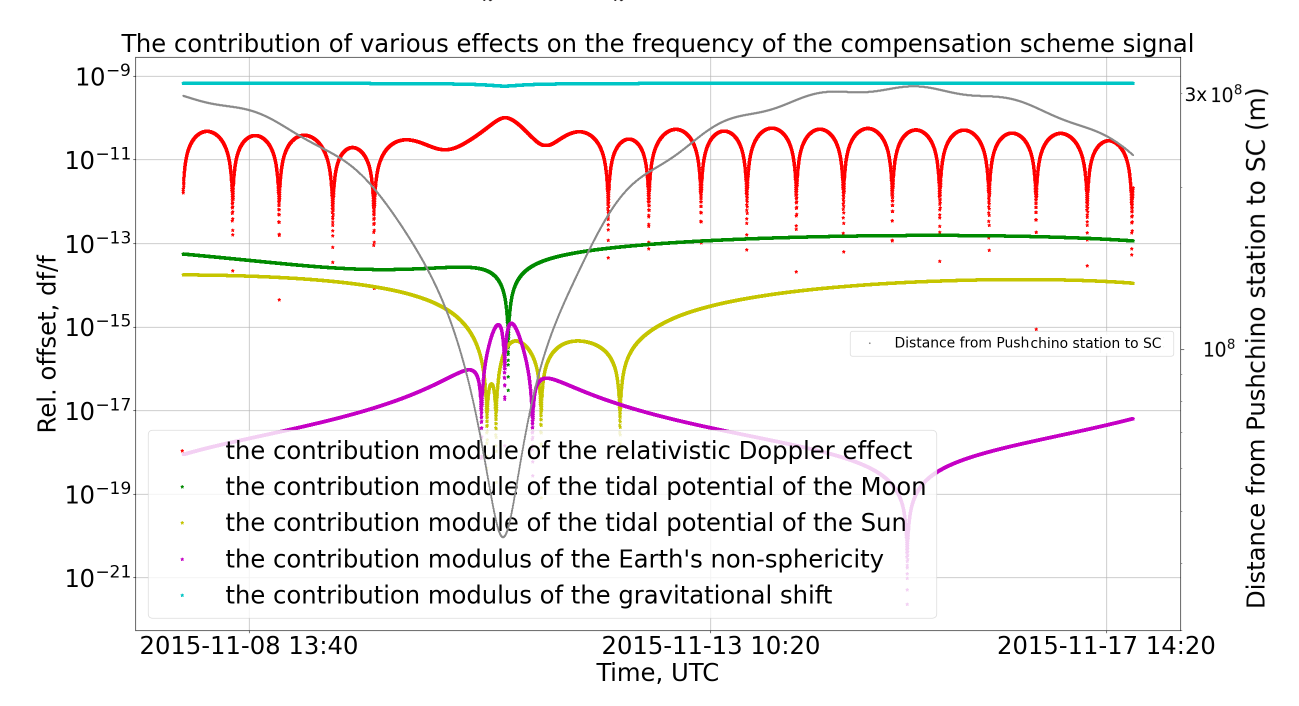


Fig. 3. Time dependence graph of the module of all calculated effects (left scale), as well as the distance between the Pushchino tracking station and the spacecraft (right scale), built using reconstructed orbit data

where e_k is the violation parameter estimate in an individual session, σ_k is the variance in an individual session, e_{opt} is the optimal estimate ε , m is the number of sessions.

This is the key "merging algorithm" that provides an optimal unbiased and efficient (minimal) estimation of the violation parameter ε across the set of measurement sessions. The variance of the value $\hat{\varepsilon}_{opt}$ is determined using Fisher's information matrix (from its parameter estimation formulas), specifically,

$$\sigma_{\varepsilon_{opt}}^2 = -\left[\left\langle \frac{\partial^2 \ln \Lambda(\hat{\varepsilon} \mid \varepsilon)}{\partial \varepsilon^2} \right\rangle \right]^{-1} = \left[\sum_{k=1}^m \frac{1}{\sigma_k^2}\right]^{-1}. \quad (8)$$

Taking into account (7) and (8), we can write the integral estimate $\hat{\varepsilon}$ as a sum of contributions from each session with their weight multipliers γ_k :

$$\hat{\varepsilon} = \sum_{k=1}^{m} \gamma_k \, \varepsilon_k, \quad \gamma_k = \left(\frac{\sigma_{min}}{\sigma_k}\right)^2, \tag{9}$$

where m is the number of sessions, σ_{\min} is the minimum value σ . It is evident that the influence of sessions with large variance is suppressed.

4. DATA PROCESSING

Data processing consisted of several sequential stages. In the first stage (preliminary filtration), the first 7 seconds of each synchronization segment 1w or 2w were removed from the session recording, where signal "capture" occurred and SNR was low (< 10³).

Further, sessions where frequency capture after mode switching took more than 15 seconds were selected, which reduced the duration of synchronized mode 1w and worsened the potential accuracy of signal frequency detection ($> 10^{-4}$ Hz), there were 17 such sessions, and they were excluded from further processing. After the preliminary filtration stage, processing followed the scheme described in Section 2 of this article. First, we compensated for the trend caused by the first-order Doppler effect (see Fig. 2 – graph slope) using compensation scheme 2, residual effects after applying the compensation scheme are shown in the graphs in Fig. 3. It should be noted that corrections for Earth's non-sphericity and Sun's tidal potential are at least an order of magnitude less than the accuracy of the frequency standards used, so these effects could be ignored. Other effects – lunar tidal potential, relativistic Doppler effect – are significant and contribute substantially to the total

Table 2. Measurements of violation parameter ε and σ_k in gravitational sessions

Session	Date	$\varepsilon_k \cdot 10^{-5}$	σ_k^2	ϵ_{weight}
raks17az	16-09-30	4.5	0.000494	1.41 e-5
raks17bl	16-12-06	6	0.003112	2.98 e-6
raks17bm	16-12-06	4.8	0.002928	2.54 e-6
raks17bo	16-12-15	4	0.002664	2.32 e-6
raks17br	17-03-12	2.1	0.000977	3.32 e-6
raks17bs	17-03-13	1.2	0.001410	1.34 e-6
raks17bt	17-03-26	3.2	0.000752	6.58 e-6
raks17bv	17-03-29	1.7	0.0029319	8.97 e-7
raks17aw	16-09-29	40	0.631962	2.45 e-7
raks17ay	16-09-29	30	0.002486	1.29 e-7
raks17bi	16-11-26	63	0.000251	1.03 e-4
raks17bk	16-12-05	34	4111	-3.05 e-8
raks17bn	16-12-14	174	0.001939	-2.78 e-5
raks17bu	17-03-29	1032	0.004340	1.10 e-4

error of the entire experiment. Compensation for these factors was carried out using the reconstructed spacecraft orbit (ballistic group of IPM RAS).

An important step in reducing systematic error in the estimation of ε is compensating for the detuning effect (frequency mismatch) between onboard and ground frequency standards (term Δ_h in equation (2)). For this purpose, data from calibration sessions conducted in parallel with gravitational sessions were used. A detailed description of the calibration sessions concept and detuning calculation results are presented in paper [19]. Detuning compensation was performed by interpolating the measured values in calibration sessions to the date of the gravitational session, after which the detuning error was subtracted similarly to other effects. For a small portion of gravitational sessions (less than 10%), the detuning remained unknown, and these sessions were excluded from processing. These were joined by sessions that had interference caused by receiving equipment, lack of correct ballistic data, and nonlinear signal frequency changes. In total, 9 sessions were excluded from processing in the second stage. As a result, the number of sessions that passed all selection criteria was 14. Their data are shown in Table 2.

Using the data obtained after processing all (Table 2) gravitational sessions in accordance with the measurement strategy, we can find the normalization coefficient α :

$$\alpha = \left(\sum_{k=1}^{m} \frac{1}{\sigma_k^2}\right)^{-1} = 0.0001547. \tag{10}$$

Further, according to formula (7), we can find ε_{opt} from the set of measurements considering the weight factor. Thus, the aggregate estimate equals $\varepsilon_{opt} = 1.57 \cdot 10^{-5}$.

Combining sample variances and finding the interval estimate according to the distribution χ^2 (see [18]), we get

$$\frac{m_k - 1}{\chi^2 (1 - \gamma)(m_k - 1)} \hat{\sigma}_k^2 \le \sigma_k^2 \le \frac{m_k - 1}{\chi^2 (1 + \gamma)(m_k - 1)} \hat{\sigma}_k^2,$$

$$\gamma = 0.95, \qquad \sigma_k^2 = 3.96 \cdot 10^{-5}.$$
(11)

Within the minimax approach, we rely only on the right side of the estimate. As a result, across all sessions, we obtain the final result:

$$\varepsilon_{opt} = (1.57 \pm 3.96) \cdot 10^{-5}.$$
 (12)

5. CONCLUSIONS

Expression (12) demonstrates the main result of gravitational sessions conducted with the RadioAstron SRT. The correspondence of experimental data measuring the RedShift effect to the GRT formula has been confirmed with increased accuracy $\approx 4 \cdot 10^{-5}$ compared to the classical level of the first space experiment GP-A: $1.4 \cdot 10^{-4}$ [5]. The relevance of such confirmation is related to the fact that the redshift effect is an integral part of Einstein's Equivalence Principle (EEP), which represents the experimental basis of GRT [2]. In particular, the universality of redshift in any space-time zone guarantees its positional invariance. Violation of such universality means rejection of GRT. In this aspect, it is important that gravitational measurements with RadioAstron for the first time included sessions at very distant ranges from Earth. Other known orbital redshift measurements were performed in the near-Earth zone with a radius of $\approx 20,000$ km, including Galileo satellites. Measurements with the latter were conducted independently by French and German groups; reports in works [6,7] showed scatter in the violation parameter within $(2.48 \div 4.5) \cdot 10^{-5}$ with an error of 1 σ . Thus, the new RadioAstron result is quite consistent with Galileo data (GREAT project). Interest in further increasing the accuracy of redshift

effect measurements is dictated by its connection with (EEP), since any violation of (EEP) opens the possibility of searching for "new physics". Evaluating the role of gravitational measurements with RA for the selection of alternative relativistic gravity theories is currently difficult. The literature mainly considered redshifts on cosmological scales (see, for example, [21]). Based on measurements in the Solar System, in principle, it is also probably possible to formulate recipes for such selection, but this would require serious additional research. Regarding the motivation for improving the accuracy of redshift measurements and its practical applications, besides the heuristic value of in-depth verification of EEP, there is an obvious navigational need for increasingly accurate calculation (prediction) of spacecraft trajectories, especially in deep space [22], where the RedShift value is incorporated in radar trajectory control (the corresponding correction was introduced by the ballistic group of IPM RAS while servicing the RA mission). Projects for more accurate redshift measurements can be found, in particular, in works [2, 6, 7, 20].

ACKNOWLEDGMENTS

The authors express their gratitude to the leadership of the "RadioAstron" group at the ASC LPI M. V. Popov and Yu. Yu. Kovalev for their constant support in working with gravitational measurements and their processing, as well as to the director of SAI MSU A. M. Cherepashchuk for attention to the topic and creating favorable working conditions for most co-authors.

REFERENCES

- **1.** *N.S. Kardashev, V.V. Khartov, V.V. Abramov et al.*, Astron. Rep. **57**, 153 (2013).
- 2. *C.M. Will*, Living Rev. Relativity 17, 4 (2014).
- **3.** A.V. Biriukov, D.A. Litvinov, and V.N. Rudenko, Astron. Rep. **58**, 783 (2014).
- **4.** *R.F.C. Vessot and M.W. Levine*. General Relativity and Gravitation **10**, 181, (1979).
- **5.** *R.F.C. Vessot, M.W. Levine, and E. M. Mattison*, Phys. Rev. Lett. **45**, 20 (1980).
- **6.** *P. Delva, N. Puchades, E. Schonemann et al.*, Phys. Rev. Lett. **121**, 231101 (2018).
- 7. S. Herrmann, F. Finke, M. Lulf et al., Phys. Rev. Lett, 12 1231102 (2018).

- **8.** *N.V. Nunes, N. Bartel, M.V. Zakhvatkin et al.*, Advances in Space Research, **65**, 790 (2020).
- **9.** *N.V. Nunes, N. Bartel, A. Belonenko et al.*, Class. Quantum Grav. **40**, 175005 (2023).
- **10.** *G. Molera Calves*, Ph. D. Dissertation, Aalto University, Pub. No **42** (2012).
- **11.** A.V. Belonenko, A.V. Gusev, and V.N. Rudenko, Gravitation and Cosmology, **27**, 383 (2021).
- **12.** A.V.Belonenko, S.M. Popov, V.N. Rudenko et al., Grav. and cosmology, **26**, 128 (2020).
- **13.** *A.V. Gusev, D.A. Litvinov, and V.N. Rudenko*, JETP **150**, 937 (2016) [A. V. Gusev, D. A. Litvinov, and V.N. Rudenko, J. Exp. Theor. Phys. **123**, 814 (2016)].
- 14. M.V. Sazhin et al., Astron. Rep. 54, 959 (2010).
- **15.** IAU SOFA Board, IAU SOFA Software Collection Issue 2021-01-25 http://www.iausofa.org

- **16.** *M.V. Zakhvatkin, A.S. Andrianov, V.Y. Avdeev et al.*, Advances in Space Research, **65**, 798 (2021).
- **17.** *A.V. Belonenko, F.S. Gurin, V.N. Rudenko et al.*, Space, Time and Fundamental Interactions. **3-4**, 3 (2023).
- **18.** *B.R. Levin*, Theoretical Foundations of Statistical Radio Engineering, **1**, 353 (1989).
- **19.** *D.A. Litvinov, V.N. Rudenko, A.V. Alakoz et al.*, Phys. Lett. A **382**, 2192 (2018).
- **20.** *D. Litvinov and S. Pilipenko*, Class. Quant. Grav. **38**, 135010 (2021).
- **21.** *D. Rosselli, F. Marulli, A. Veropalumbo*, Astron. Astrophys. **669**, (2023).
- **22.** *P.C. Brandt, E.A. Provornikova, A. Cocoros et al.*, Acta Astronautica **199**, 364 (2022).